# Using Three-Dimensional Finite Element Models and Principles of Active Muscle Contraction to Analyse the Movement of the Tongue

**M.-C. Wu[1], J.-C. Han[2], O. Röhrle[2], W. Thorpe[2], P. Nielsen[1,2]**

[1]The Department of Engineering Science, [2]The Bioengineering Institute
University of Auckland, New Zealand
mwu035@ec.auckland.ac.nz

## Abstract

This paper presents an anatomically-based three-dimensional computational model of the human tongue. It uses a large deformation finite element method that incorporates active contractile effects of the tongue's muscles to simulate its movement. The model provides an anatomically-based framework, which is capable of simulating the tongue's kinematics during speech production or normal mastication. This paper describes in particular, the processes of creating a Finite Element volume mesh, the procedure of fitting the tongue's muscle fibres, and the development of a constitutive description, which mimics physiological properties of passive and active muscle mechanics by adding active contractile stress. Furthermore, it investigates the effects of activating different muscle groups, in particular the effects of the interdependency between muscle pairs, and their overall contribution to the complex deformation patterns of the tongue.

## 1. Introduction

The tongue is a dextrous organ. Because of its complicated structure and shape, and its limited visibility, its biomechanical behaviour is relatively poorly understood. However, its complex muscular fibre structure makes it virtually impossible to predict its deformation and movement without a computational model. Since the tongue's movement is clinically often directly linked to difficulties in speech, it is highly desirable to have a computational model that assists one in developing a better understanding of its mechanical behaviour.

Several models of the tongue have previously been proposed (Wilhelms-Tricarico, 1995; Dang & Honda, 2001 ; 2004). Most of these tongue models however focus only on different approaches to reconstruct the surface of the tongue. Full three-dimensional models that incorporate its complex muscle structure and its biomechanical properties in order to study its movements are rare. The most advanced and sophisticated model was introduced by Wilhelms-Tricarico already in 1995 (Wilhelms-Tricarico, 1995).

The challenging part in modelling the movement of the tongue is its complex construct and its interaction of different muscles. In general, the tongue's muscles can be separated into two different groups according to their origins: the intrinsic muscles and extrinsic muscles. The intrinsic muscles have both their origins and terminations within the tongue while the extrinsic muscles arise from outside of the tongue and terminate inside. In order to develop a realistic model of the tongue, it is important to determine the direction and location of different muscles within the tongue. This, however, is an extremely complex and challenging task. In the past, there have been a few studies using different methods to determine the location and distribution of the muscles (Wilhelms–Tricarico, 2005; Takemoto, 2001). In Wilhelms–Tricarico (2005), the Visible Human female data set and anatomical literature on the tongue is used to work out a description of the different muscle groups. The data is incorporated into a finite element (FE) model of the tongue consisting of 250 tri-quadratic Finite Elements (Wilhelms-Tricarico, 2005; Data of the tongue 2005). From this data set, the superior longitudinal, inferior longitudinal, tranversus and verticalis muscle (intrinsic muscles), and the genioglossus, hyoglossus and styloglossus muscle muscle (extrinsic muscle) fibres are extracted and form the basis of the work reported here.

This paper uses an FE model with cubic Hermite Finite element basis functions. Such basis functions have the advantage that they exhibit not only nodal continuity, but also continuity in its first derivatives. The key advantages of such elements, over elements that only enforce nodal continuity, are that they enforce stress continuity and that often a relative small amount of elements is sufficient to represent complex geometrical shapes such as the ones arising frequently in modelling organs. This type of element should pose a significant improvement over using standard tri-linear or tri-quadratic elements.

## 2. Constructing the Tongue Model

The Bioengineering Institute at the University of Auckland is part of the Physiome project that aims to provide a comprehensive framework for modelling the human body using computational methods (Hunter & Borg, 2003). As part of this ambitious goal, there have been attempts in the past to construct an FE model of the tongue. However, the initial model developed in 2005 was based on the sagittal and coronal slices of the Visible Human database of the male cadaver. Since the muscle fibre data is for the female Visible Human, it was necessary to modify the male model in such a way that it corresponds to the female one. Furthermore,

Proceedings of the 11th Australian International Conference on Speech Science & Technology, ed. Paul Warren & Catherine I. Watson. ISBN 0 9581946 2 9
University of Auckland, New Zealand. December 6-8, 2006. 

Accepted after abstract only review

previous models were lacking any internal structure. This section explains the method how this initial tongue model, which consisted of 10 tri-cubic Hermite elements (1 element in the x-direction, 2 elements in the y-direction and 5 elements in the z-direction), is used to construct a fully three-dimensional biomechanical model capable of representing the tongue's movement based on activating different muscle groups. This method can be broken up into the following steps:

1. Refitting of the FE volume mesh.
2. Incorporating the data from fibre directions within the FE mesh by means of fitting.
3. Defining a constitutive law, in the muscle fibre coordinate system, capable of capturing components of active and passive muscle behaviour.
4. Solving the continuum-based equations of finite elasticity using the above model, constitutive law, and boundary conditions.

## 2.1. Finite Element basics

All simulations within this paper are carried out with the software package CMISS, which is developed at the Bioengineering Institute in Auckland. This modelling software package is designed for Finite Element, boundary element, and collocation techniques for a variety of complex bioengineering problems. It consists of a number of modules including a open source graphical front end (CMGUI) tool with advanced 3D display, and a computational backend (CM) that may be run remotely on powerful workstations or supercomputers (CMISS, 2006).

The 3D volume mesh of the tongue and the muscle groups are interpolated using cubic Hermite basis function (Fig. 1). Cubic Hermite basis functions ensures in addition to the continuity of the nodal values that the first derivative with respect to a normalised element coordinate system (Fernandez, 2004), $\xi$, is continuous across element boundaries. In contrast, linear Lagrange basis functions only ensure continuity of nodal values between elements. As already earlier mentioned, the cubic Hermite basis functions have also advantages in FE modelling of biological bodies since often only a few elements are necessary to accurately represent complex biological shapes. Furthermore, the continuity of the first derivatives ensures strain continuity for elasticity problems.

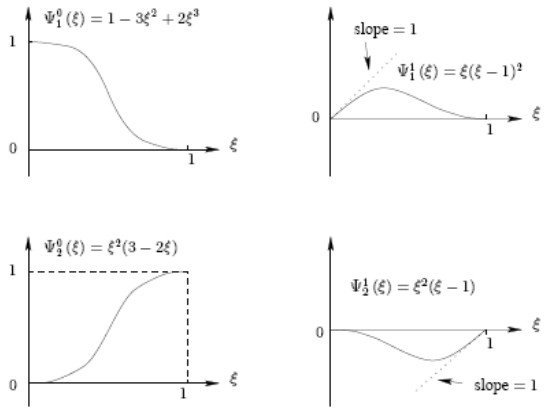


*Figure 1:* Cubic Hermite basis functions.

## 2.2. Step 1: Refitting the Volume Mesh

The fitting procedure is based on a data point cloud and an initial volume/surface mesh. The data point cloud is obtained by redigitizing the surface of the Visible Human female tongue. For this purpose, the boundaries of the tongue's surface on the sagittal and coronal slices of the Visible Human data set has been traced by hand. Then, the previous model of the tongue (the one from the Visible Human male) is used as an initial guess for the current one. (Note that any other initial guess, even a crude tri-linear FE mesh, would have worked in the same way.) Then, a fitting procedure, which is described in more detail below, is used to construct the volume mesh of the Visible Human female.

The fitting procedure is based on an objective function, given by

$$F(u_n(\xi_{1d},\xi_{2d})) = \sum_{d=1}^{N} w_d \left\| u_n(\xi_{1d},\xi_{2d}) - z_d \right\|^2 + F_s(u_n(\xi_{1d},\xi_{2d})) \quad , \quad (1)$$

which can be split up into two components: the data error and the smoothing constraint. The first part, the error constraint, minimizes the distance of the orthogonal projection of each data point onto the FE surface mesh. The second part controls the smoothness of the surface. In (1), the mesh surface point, at which its normal vector passes through data point $z_d$, is denoted by $u_n(\xi_{1d},\xi_{2d})$, where $(\xi_{1d},\xi_{2d})$ are local element coordinates, $w_d$ a weight for each data point, and $N$ the total number of data points. The smoothing constraint, $F_s(u_n(\xi_{1d},\xi_{2d}))$, is a so-called Sobolev smoothing penalty function and is given below:

$$F_s(u_n(\xi_{1d},\xi_{2d})) = \int_0^1\int_0^1 \left[ \alpha_1 \left\| \frac{\partial u}{\partial \xi_1} \right\|^2 + \alpha_2 \left\| \frac{\partial u}{\partial \xi_2} \right\|^2 + \alpha_{11} \left\| \frac{\partial^2 u}{\partial \xi_1^2} \right\|^2 + \alpha_{22} \left\| \frac{\partial^2 u}{\partial \xi_2^2} \right\|^2 + \alpha_{12} \left\| \frac{\partial^2 u}{\partial \xi_1 \partial \xi_2} \right\|^2 \right] \partial\xi_1 \partial\xi_2 \quad (2)$$

where the $\alpha_i$'s are additional wrights which control the smoothing. The subscripted $n$ indicates that this procedure of finding the optimal surface shape is an iterative process.

The result of using this method is depicted in Fig 2, in which the dots represent the data points obtained by the digitization process. Note that this methodology can also be used for customizing or morphing this generic tongue model to a patient specific one.

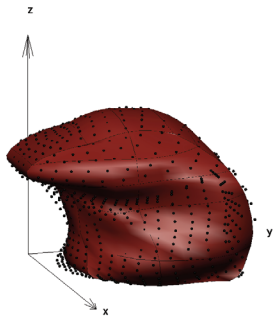


*Figure 2:* Static tongue model.

Proceedings of the 11th Australian International Conference on Speech Science & Technology, ed. Paul Warren & Catherine I. Watson. ISBN 0 9581946 2 9
University of Auckland, New Zealand. December 6-8, 2006. 

Accepted after abstract only review

## 2.3. Step 2: Representation of Fibre Direction using Fibre Angle and Imbrication Angle

To use the description of the fibre orientation within CMISS, it is necessary to define a field within each element that describes the global fibre field orientation and can be approximated by basis functions associated with parameters defined at the element nodes (Nielsen, Grice, Smaill & Hunter , 1991). To do so, the fibre direction, which is stored as three unit vectors at 96750 different data points within the fitted volume mesh, must be converted into two angles. For this purpose, a muscle fibre direction is represented in 3D by one angle that ranges from 0 to 360 degrees in one plane and by another angle that ranges from -90 to 90 degree in another plane. Here, the assumption is that the fibre angle ranges from 0 to 360 degree in the xy-plane and that the imbrication angle ranges from -90 to 90 degree in the plane spanned by the direction of the orthogonal projection onto the xy-plane and the z-direction (comp. Fig. 3). These variables are then used to fit (in a similar fitting procedure as described above) to a field, which is defined at the nodal points of the volume mesh and interpolated with cubic Hermite basis functions.

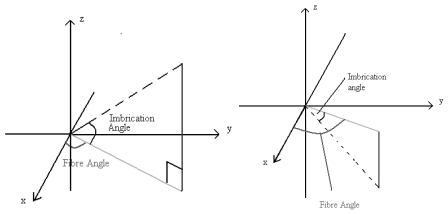


*Figure 3:* Definition of the fibre and a positive (Left) and negative (Right) imbrication angle.

## 2.4. Step 3: A Constitutive law with components of active and passive muscle behaviour.

Biological soft tissues that undergo large deformations, e.g. the tongue, are mathematically best modelled by the governing equations of finite elasticity. A crucial part of finite elasticity theory is the constitutive law, which describes the mechanical behaviour of the respective soft tissue. For this study, a Mooney-Rivlin material law, which is under the action of applied forces highly elastic, incompressible, and isotropic (Rivlin, 1951), is modified to a transversely isotropic material law by incorporating components of passive and active muscle behaviour (Röhrle & Pullan, 2006).

The tongue with its multi-directional fibre arrangement is an anisotropic material. However, it can be assumed that it exhibits transversely isotropic material properties with respect to a particular muscle. Hence, each muscle within the tongue is modelled with an elastic, incompressible, and transversely isotropic material. This transversely isotropic property is obtained by enhancing the stress tensor of a Mooney-Rivlin material by adding additional stress components with respect to the fibre direction. These additional components stem from passive and active responses along the fibre direction in order to increase the stiffness in that particular direction.

Hyper-elastic constitutive laws can be derived mathematically by postulating a strain energy function, W, which can be seen as a scalar potential that depends on the components of either the Green's strain tensor, E, the Cauchy-Green deformation tensor, C, or its invariants. The strain energy function for a Mooney-Rivlin material is given by

$$W(I_1, I_2, I_3) = \overline{W}(I_1, I_2) + \kappa(I_3 - 1) \tag{4}$$

with

$$(I1,I2) = c1(I1-3) + c2(I2-3), \tag{5}$$

where I1-I3 are the isotropic invariants, κ is a scalar that, under certain circumstances, can be associated with the hydrostatic pressure. (To enforce incompressibility, the strain energy function, $\boldsymbol{W}$, is separated into two parts – a deviatoric and a hydrostatic part. Then, $\boldsymbol{W}$, can be expressed in terms of the distortional component of the right Cauchy-Green tensor $\widetilde{C} = J^{-2/3}C$, where J is the determinant of F, or its respective invariants. Then, κ can be associated with the hydrostatic pressure and $\kappa = -\frac{1}{2}p,$). The components of the stress tensor are obtained from the strain energy function by differentiating (4) with respect to the components of the Green's strain tensor. Since everything is assumed to be aligned with a material coordinate system (the fibre direction), the components of the Green strain tensor are denoted with, $E_{\alpha\beta}$ (for more details on introducing a material coordinate system see (Nash & Hunter, 2000)). Hence, the second Piola-Kirchhoff stress tensor is given by

$$T_{iso}^{\alpha\beta} = \frac{\overline{W}(\widetilde{I}_1, \widetilde{I}_2)}{\partial E_{\alpha\beta}} - p\delta^{\alpha\beta}, \tag{6}$$

where $\alpha$ and $\beta$ are with respect to the fibre direction ($f$) or its transverse directions ($s,n$) and $\delta_{\alpha\beta}$ the Kronecker delta.

Under the assumption that the passive resistance grows in fibre direction $f$ only with respect to the fibre stretch $\lambda$, where $\lambda = \sqrt{2E_{ff} + 1}$, a true (Cauchy) stress tensor, mapped to the reference configuration, can be added to the Piola-Kirchhoff stress tensor:

$$T_{passive}^{\alpha\beta} = T_{iso}^{\alpha\beta} + J(\sigma_{passive}^{ff} f_{passive}^{fibre}(\lambda)) \frac{\partial X^{\alpha}}{\partial v_f} \frac{\partial X^{\beta}}{\partial v_f}, \tag{7}$$

where $f_{passive}^{ff}(\lambda)$ is a normalized force which depends on the fibre stretch and $\sigma_{passive}^{ff}$ is the maximal passive tensile stress, which itself is a Cauchy stress, such that the product equals the additional stress induced from stretching the object in the f-direction, and $\frac{\partial X^M}{\partial v_f}$ is the inverse of the deformation tensor with respect to f-component of the material coordinate system. The function $f_{passive}^{fibre}(\lambda)$ is defined by

$$f_{passive}^{fibre}(\lambda) = \begin{cases} 0, & \lambda \le 1, \\ P_1(e^{P_2(\lambda-1)} - 1), & 1 < \lambda \le \lambda_{ofl}, \\ P_3\lambda + P_4, & \lambda > \lambda_{ofl}, \end{cases} \tag{8}$$

and is depicted in Fig. 4. Constants $P_1$, $P_2$, $P_3$, $P_4$, and the optimal fibre stretch length, $\lambda_{ofl}$ are listed in Table 1. Similar to the passive stress tensor, one enhances $T_{passive}^{\alpha\beta}$ by its active component, such that

$$T_{active}^{\alpha\beta} = T_{passive}^{\alpha\beta} + + J(\alpha\sigma_{active}^{ff} f_{active}^{fibre}(\lambda)) \frac{\partial X^{\alpha}}{\partial v_f} \frac{\partial X^{\beta}}{\partial v_f}, \tag{9}$$

where the parameter $\alpha$, the level of activation, which controls the amount of active stress. The active stress is computed by

Proceedings of the 11th Australian International Conference on Speech Science & Technology, ed. Paul Warren & Catherine I. Watson. ISBN 0 9581946 2 9
University of Auckland, New Zealand. December 6-8, 2006. 

Accepted after abstract only review

multiplying the maximal active tensile stress, $\sigma^{ff}_{active}$, with the normalized active force,

$$f^{fibre}_{active}(\lambda) = \begin{cases} -\frac{25}{4\lambda^2_{ofl}}\lambda^2 + \frac{25}{2\lambda_{ofl}}\lambda - 5.25 & 0.6\lambda_{ofl} \le \lambda \le 1.4\lambda_{ofl} \\ 0 & otherwise. \end{cases} \quad (10)$$

This function is constructed in such a way that it has a value of 1 at optimal fibre length stretch $\lambda_{ofl}$, and 0 when the fibre stretch values are smaller than 0.6 $\lambda_{ofl}$ or greater than 1.4 $\lambda_{ofl}$ (see Fig. 4). The values of the constants used to define the constitutive relation are shown in Table 1.

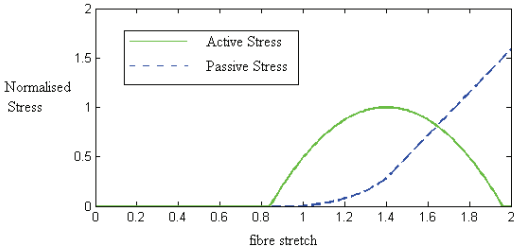


*Figure 4:* Normalised stress versus fibre stretch of the active and passive component (Röhrle & Pullan, 2006).

| Constant | Value |
|---|---|
| $c_1$ | 0.01 MPa |
| $c_2$ | 0.01 MPa |
| $P_1$ | 0.05 |
| $P_2$ | 6.6 |
| $P_3$ | 2.1751 |
| $P_4$ | -2.7655 |
| $\sigma^{ff}_{passive}$ | 0.3 MPa |
| $\sigma^{ff}_{active}$ | 0.3 MPa |
| $\lambda_{ofl}$ | 1.4 |

*Table 1:* Values of the constants in $f^{fibre}_{active}(\lambda)$ and $f^{fibre}_{passive}(\lambda)$.

### 2.5. Step 4: Boundary Condition and FEM solution process

The bottom of the tongue is connected to the hyoid bone and the jaw (Iny & Levine, 2000). These attachments at the bottom of the tongue affect the movement of the tongue caused by the activated extrinsic muscles. Hence, all nodal values, and the derivatives associated with the surface are fixed and implemented as Dirichlet boundary (Type I) conditions as shown in Fig. 5.

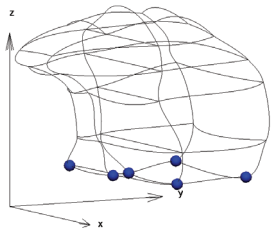


*Figure 5:* Six nodal points (Blue) are fixed at their original position

Then, the motion of the tongue is obtained by varying the level of activation, $\alpha$, linearly between 0 and 1. For each increase of the activation level, a Galerkin Finite Element method with cubic Hermite basis functions is used to solve the continuum-based equations of finite elasticity.

## 3. Results

### 3.1. Activation of the transversus muscle

To observe the effects of different active contractile stress on the movement of the tongue, the deformations of the tongue are calculated after altering the activation levels for the transversus muscle ($\alpha = 0$, $\alpha = 0.25$, $\alpha = 0.5$, $\alpha = 0.75$, and $\alpha = 1.0$, Fig. 6). As the transversus muscle contracts toward the middle on the frontal plane, the tissue of the tongue must extend forward in order to preserve the volume of the tongue body.

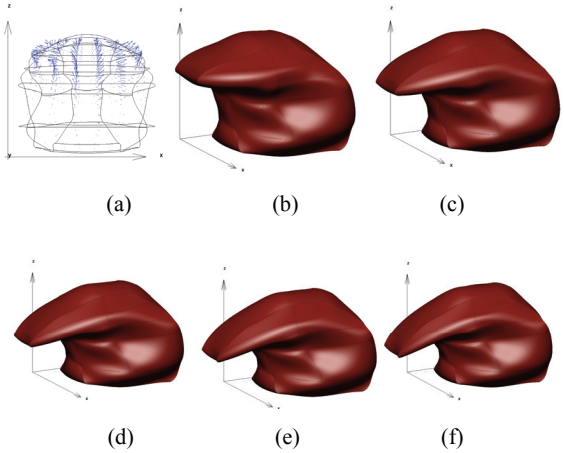


*Figure 6: (a)* Direction of the transversus fibre; and Movement of the tongue when the level of activation value $\alpha$ is set to (b) 0, (c) 0.25, (d) 0.5, (e) 0.75 and (f) 1.0.

It also appears that, as the contractile stress increases, the rate of strain decreases. As previously the tongue becomes stiffer as the strain of the material increases. This can be seen by plotting the displacement of a nodal point versus the level of activation (active contractile stress) (Fig. 7).

Proceedings of the 11th Australian International Conference on Speech Science & Technology, ed. Paul Warren & Catherine I. Watson. ISBN 0 9581946 2 9
University of Auckland, New Zealand. December 6-8, 2006. 

Accepted after abstract only review

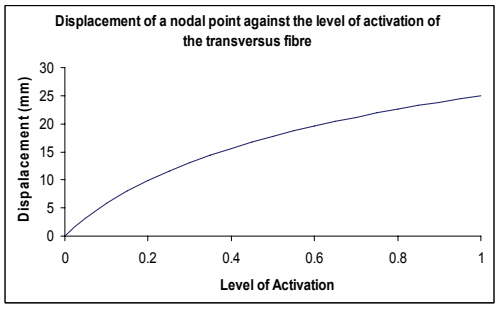


*Figure 7:* Displacement of a nodal point plotted against the activation level of the transversus muscle.

Fig. 7 shows that, as the level of activation increases, the displacement of a nodal point on the tongue also increases. However, the rate of strain deceases as the level of activation increases. This illustrates that a higher stress is required to perform the same amount of deformation after the material is already stretched by a certain amount, thus indicating that the tongue tip has indeed became stiffer.

## 3.2. Activation of different muscle groups

This section describes the movement caused by each intrinsic and extrinsic muscle by solving for different activation levels. The calculated movement for each individual muscle is compared to the movement of the tongue shown in the Human Tongue Atlas and predicted by Dang & Honda, (2001 ; 2004).

### *3.2.1. Superior longitudinal muscle*

The superior longitudinal (SL) muscle is believed to cause dorsiflexion of the tongue. The SL muscle is located on the superior surface of the tongue and is pointing forward and deforms the tongue in the expected way and is depicted in Fig. 8a. Probably due to the optimization techniques used to fit the FE mesh, it appears that the volume mesh is not exactly symmetric to the sagittal plane and causes a slightly asymmetric contraction. However, this error is not significant. The deformation pattern can still be recognised.

### *3.2.2. Inferior longitudinal muscle*

The inferior longitudinal muscle is expected to shorten the tongue and causes the tongue tip to move downward (Fig. 8b). The simulations indeed demonstrate that activating the inferior longitudinal muscle causes the tongue to shorten by rising slightly and that the tongue tip moves, as expected, downwards.

### *3.2.3. Verticalis muscle*

The fibres of the verticalis muscle are located vertically and are expected to flatten and to protrude the tongue tip out (Fig. 8c). The movement of the tongue model seems reasonable, although, again, there seems to be a slight asymmetrical deformation between the left and right hand side of the tongue.

### *3.2.4. Hyoglossus muscle*

It is believed that the hyoglossus muscle causes retrusion of the tongue. The model demonstrates that the tongue moves by a small amount backwards and that a pull-down of the posterior part of the tongue causes the tongue tip to move up (Fig. 8d). The deformation pattern of this model is similar to the one in (Dang & Honda, 2004).

### *3.2.5. Genioglossus muscle*

Contraction of the genioglossus muscle can result in various different movements, e.g. ventroflexion, depression, retrusion and protrusion (Human Tongue Atlas). As the muscle is modelled into two separate compartments, their corresponding movement will also be discussed separately.

The model shows that the anterior part of the genioglossus muscle causes slight ventroflexion, depression, and a slight protrusion. Compared to the model in (Dang & Honda, 2001) the results presented in this paper (Fig. 8e) shows that the posterior part of the tongue does apparently not depress as strongly.

The posterior part of the genioglossus muscle is believed to cause elevation. The deformation caused by activating that part of the muscle in this model is similar to that shown in (Dang & Honda, 2001 ; 2004). Both models show that activating the posterior part of genioglossus muscle results in an elevation of the posterior part of the tongue and slight protrusion of the tongue's anterior part (Fig. 8f).

### *3.2.6. Styloglossus muscle*

The styloglossus muscle is expected to cause retrusion and elevation of the lateral margion of the tongue. Similar to the genioglossus muscle, this muscle is separated into the anterior part and posterior part.

The anterior part of styloglossus muscle causes a slight elevation of the tongue body. The deformed shape of the tongue is very similar to the deformation caused by inferior longitudinal muscle (Fig. 8g). The posterior part of styloglossus muscle causes contraction at the posterior part of the tongue base in transverse direction and, as a result, the tongue tip is lifted up (Fig 8h).

### *3.2.7. Digastric, mylohyoid and geniohyoid muscle*

These three muscles are located on the outside and below the tongue; they mainly change the position of the tongue base and cause no change in shape of the visible part of the tongue.

The digastric muscle is the most inferior muscle of all the muscle groups modeled. Its activation causes the whole tongue to elevate (8i). Activation of the mylohyoid causes a reduction in thickness of the lower tongue body at the transverse plane and hence results in retrusion and elevation (8j). The geniohyoid muscle is located just above the digastric muscle with almost the same direction of contraction. Therefore, these two muscles have similar patterns of deformation (8k).

### *3.2.8. Combined effect of the anterior part of genioglossus and the verticalis muscle*

The anterior part of the genioglossus and the verticalis muscle are chosen to be activated at the same time as an example for muscles, which are spatially separated and cause very distinctive deformations. As discussed in the previous section, the anterior genioglossus muscle causes ventroflexion and the verticalis muscle causes protrusion of the tongue tip. Activated at the same time (with the same level of activation) results in a combined ventroflexion and protrusion movement (Fig 8(l)).

Proceedings of the 11th Australian International Conference on Speech Science & Technology, ed. Paul Warren & Catherine I. Watson. ISBN 0 9581946 2 9
University of Auckland, New Zealand. December 6-8, 2006. 

Accepted after abstract only review

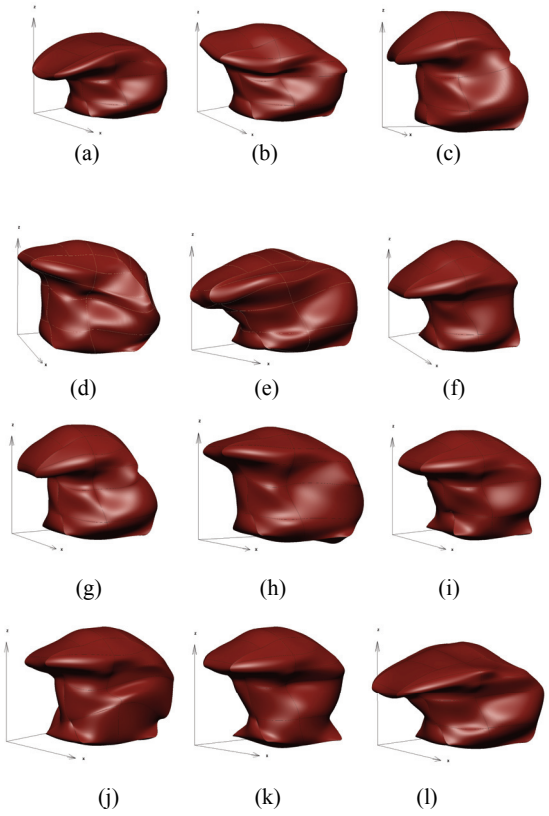


*Figure 8:* Deformation caused by different muscle group: (a) verticalis (b) superior longitudinal, (c) inferior longitudinal, (d) hyoglossus, (e) anterior, (f) posterior part of genioglossus, (g) anterior part of styloglossus, (h) posterior part of styloglossus, (i) digastric, (j) hyoglossus, (k) geniohyoid and (l) the combined effect of the of contraction of anterior genioglossus and verticalis.

## 4. Discussion

This paper analyses the basic movements of the tongue by simulating the activation of one or multiple muscle groups in the tongue using a biomechanical computer model of the tongue. The volume mesh and the fibre directions are derived by an iterative optimization procedure that fits mesh to data sets obtained from the female Visible Human. It should be remarked that fibres, which do not occupy much of an element, for example the superior longitudinal and anterior part of styloglossus muscle, showed some discrepancies in movement compared to verticalis muscle. The reason for this is probably that the some muscles occupy a relatively small fraction of an element within the mesh and hence are not well approximated by the choice of the FE basis functions. This, however, is a consequence of choosing relatively large elements to represent the tongue.

Future work on the tongue model will involve some modifications of the CMISS software to improve the representation of the muscular fibre field, in particular, when several muscles within one element. Also, in the next step, contact mechanics needs to be considered as the movement of the tongue is constrained by its neighbouring tissues, e.g. teeth, the soft and hard palates, and the pharyngeal wall. Moreover, the model should be improved by applying more realistic boundary conditions like the ones proposed in (Dang & Honda, 2004). This, and a refined model of the mesh, should be a significant improvement towards more practical and realistic deformation patterns and movements of the tongue within the oral cavity. Both are certainly necessary for potential applications as a clinical diagnostic tool for speech disorders or mastication can be explored.

## 5. Acknowledgements

A part of the study was performed by June-Chiew Han as part of a project in 2005. The authors would like to thank the Bioengineering Institute for funding to attend the conference.

## 6. References

CMISS, The Bioengineering Institute, University of Auckland, http://www.cmiss.org .

Dang, J., & Honda, K. (2001) A physiological articulatory model for simulating speech production process. *Acoust. Sci. & Tech., 22, 6.*

Dang, J., & Honda, K. (2004) . Construction and control of a physiological articulatory model. *J. Acoust. Soc. Am. 115:853-870.*

Data of the tongue (2005), Wilhelms-Tricarico. Retrieved April 6, 2006 from http://webpages.charter.net/ reinerwt/themodel.htm#tonguemodel

Fernandez, J.W. (2004) An Anatomically Based Finite Element Model of Patella Articulation: Towards a Diagnostic Tool. *PhD thesis, the University of Auckland, New Zealand.*

Human Tongue Atlas. Retrieved April 2, 2006 from http://www.upperairway.com/tongueatlas.htm

Hunter, P.J., & Borg, T.K. (2003), Integration from proteins to organs: the Physiome Project, *Nat Rev Mol Cell Biol., 4(3):237-43*

Iny, D., & Levine, W.S. (2000), A Simplified Model for Motion Reconstruction for the Human Tongue. Dept. of Electrical Engineering, University of Maryland, USA.

Nash, M., & Hunter, P., (2000). Computational mechanics of the heart. from tissue structure to ventricular function. *Journal of Elasticity 61, 113–141.*

Nielsen, P. M., Grice, I. J. L., Smaill, B. H., & Hunter, P. J., (1991) Mathematical model of geometry and fibrous structure of the heart. *Am J Physiol Heart Circ Physiol 260 (4), 1365–H1378.*

Rivlin, R.S. & Saunders D.W. (1951), Large Elastic Deformations of Isotropic Materials. VII. *Phil Transactions of the Royal Society of London, series A*, 243, 251-288.

Röhrle, O., & Pullan, A.J. (2006) Three-dimensional finite element analysis of muscle forces during mastication. Submitted to *the Journal of Biomechanics*.

Takemoto, H. (2001) Morphological Analyses of the Human Tongue Musculature for Three-Dimensional Modeling. *Journal of Speech, Language, and Hearing Research, Vol 44, 95-107.*

Wilhelms-Tricarico, R. (1995) Physiological modeling of speech production: Methods for modeling soft-tissue articulators. *J. Acoust. Soc. Am, 97 (5), 3085-3098.*

Wilhelms-Tricarico, R. (2005) Geometric Representation of a Human Tongue for Computational Biomechanical Modelling. Research Laboratories of Electronics, M.I.T, Cambridge, Massachusetts. Retrieved April 5, 2006 from http://webpages.charter.net/reinerwt/JSHLRmanuscript.pdf